Comparison of Methods for Efficient Static Wind Tunnel Testing Using Multiple Control Surfaces

Jared A. Grauer* and Benjamin M. Simmons†
NASA Langley Research Center, Hampton, Virginia, 23681

Nhan T. Nguyen‡
NASA Ames Research Center, Moffett Field, CA 94035

Christopher J. Forte§
KBR Wyle, Inc., Moffett Field, CA 94035

John F. Quindlen¶
Boeing Technology Innovation, Huntington Beach, CA, 92647

The Integrated Adaptive Wing Technology Maturation (IAWTM) half-span wind tunnel test article was tested in the Transonic Dynamics Tunnel (TDT) at NASA's Langley Research Center in Hampton, VA. The test article has a wing aspect ratio of 13.5, wing half span length of 12.75 ft, and is configured similar to a transport aircraft. Static tests were performed to determine the nondimensional aerodynamic force and moment contributions from each of the 10 control surfaces over a range of deflection angles. Three different tests were used to obtain these data: conventional one factor at a time (OFAT) tests, design of experiment (DOE) tests, and quasi-steady sinusoid (QS2) tests. This paper presents the three approaches, and compares and contrasts the results. For the test data examined, analysis of all three tests determined statistically similar models. However, the DOE and QS2 tests were more efficient and had the possibility of determining interaction effects.

Nomenclature

C_D, C_Y, C_L	=	nondimensional drag, side force, and lift coefficients
C_l, C_m, C_n	=	nondimensional roll, pitch, and yaw moments
$E[.]$	=	expectation operator
δ_i	=	control surface deflection for $i = 1, 2, \ldots, 10$, rad or deg

Superscripts

^{T}	=	transpose
$^{-1}$	=	inverse
$\hat{}$	=	estimated value

*Research Aerospace Engineer, Dynamic Systems and Control Branch, MS 410; jared.a.grauer@nasa.gov. Associate Fellow AIAA.
†Research Aerospace Engineer, Flight Dynamics Branch, MS 410; benjamin.m.simmons@nasa.gov. Member AIAA.
‡Senior Research Scientist, Technical Group Lead, Intelligent Systems Division, MS 269; nhan.t.nguyen@nasa.gov. Associate Fellow AIAA.
§Aerospace Engineer, Intelligent System Division; christopher.j.forte@nasa.gov. Member AIAA.
¶Guidance, Navigation, & Control Engineer, Flight and Vehicle Technology; john.f.quindlen@boeing.com. Member AIAA.

I. Introduction

The NASA Advanced Air Transport Technology (AATT) project aims to develop concepts and technologies that improve the energy efficiency and lessen the environmental impact of fixed-wing transport aircraft [1]. One current effort within AATT is the Integrated Adaptive Wing Technology Maturation (IAWTM) sub-project, which is a collaboration involving multiple NASA centers and Boeing [2, 3]. Goals of the project include developing an ultra-high aspect ratio wing with a cantilever design and mature adaptive wing technologies for real-time drag reduction, gust and maneuver load alleviation, and active flutter suppression. The wind tunnel test article is a side wall-mounted, half-span test article based on the NASA Common Research Model (CRM) [4] but with an increased wing aspect ratio and flow-through engine nacelle.

Part of the research plan for the IAWTM sub-project included static tests to determine aerodynamic forces and moments due to control surface deflections. The IAWTM has 10 control surfaces, which is a relatively large number, but not as large as other vehicles recently tested at NASA Langley Research Center (LaRC) [5, 6]. As traditional one-factor-at-a-time (OFAT) tests are common but require relatively large amounts of test time, the use of design of experiments (DOE) testing was also considered. In addition, a third type of test where control surfaces are moved slowly but continuously, and herein called quasi-steady sinusoids (QS2) testing, was also considered.

All three tests were performed during testing of the IAWTM. This paper considers tests for one condition, at Mach 0.55 and dynamic pressure 103 lbf/ft^2, and compares and contrasts the results obtained from the three different static tests. The results are preliminary; other analyses and similar test data for higher angles of attack and different tunnel conditions will be examined in the future.

This paper is organized as the following. Section II describes the test article and the wind tunnel. Section III presents the three approaches for static testing. Section IV describes the results and provides discussion. Section V concludes the discussion. An appendix is included to discuss analysis techniques used in this report. Software for these algorithms come from the package System IDentification Programs for AirCraft (SIDPAC), which is available through the NASA Software Catalog [7]. Theoretical development for these techniques are presented in Ref. [8].

II. Subject Test Article and Wind Tunnel

Figure 1 shows the IAWTM test article mounted in the test section of the Transonic Dynamics Tunnel (TDT) at NASA Langley Research Center. The test article is a wall-mounted, half-span model of a transport configuration airplane. The design was based on the NASA Common Research Model (CRM) [4] but with an increased wing aspect ratio, shortened fuselage, and a flow-through engine nacelle. There is no tail section and no landing gear. It weighs about 1800 lbf and has a 13.3 ft fuselage length, 12.75 ft wing (half) span distance, 2.04 ft mean aerodynamic chord, 24.09 ft^2 (half) wing reference area, and 13.5 wing aspect ratio.

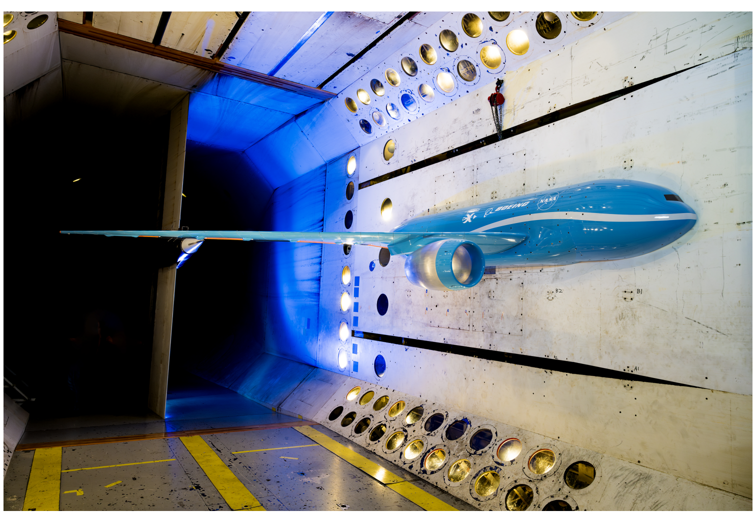

Fig. 1 Installed test article (credit: NASA / Mark Knopp).

Figure 2 shows a cut-away drawing of the test article with annotations. There are 10 control surfaces. Three ailerons, which are labeled AILA, AILB, and AILC, are located behind the engine and at the wing tip. These surfaces were powered by hydraulic actuators and had higher dynamic bandwidths and hinge moment limits. The remaining seven surfaces are miniature plain flaps (MPFs) and labeled MPFA through MPFG from the wing root towards the wing tip. These surfaces were powered by electric servo motors and had lower bandwidths and hinge moment limits. Maximum control surface deflection angles were scheduled with the tunnel condition. The sign convention used for all surfaces is that trailing-edge down (TED) is a positive deflection.

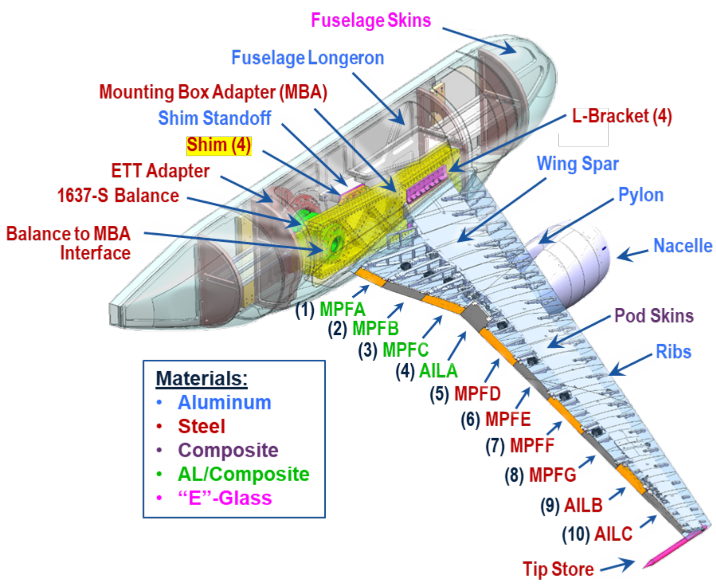

Fig. 2 Test article drawing showing control surfaces and numbering.

For the data used in this paper, the tip store (seen in Fig. 2) was not installed at the wing tip. This tip store was added during flutter testing to destabilize the test article by shifting the flutter boundary inside the test envelope. Also, mechanisms inside the fuselage were configured to connect the test article load path to the tunnel balance for measuring forces and moments. The balance was disconnected in other dynamic tests for the IAWTM test article.

Tests were performed in the TDT at NASA LaRC in Hampton, VA. The first wind tunnel entry was conducted during July–August 2024 and was primarily for model characterization, whereas the second entry was conducted during June–July 2025 for closed-loop testing. Figure 1 shows the test article mounted in the TDT test section, which has a cross-section of 16 ft by 16 ft with cropped corners. The tunnel can be filled with heavy gas R-134a (as was done during these tests), and can run up to Mach number 1.2 and a Reynolds number of 10×10^6.

More information on the IAWTM project and wind tunnel test article can be found in Refs. [2, 3]. More information on the tunnel and capabilities can be found in Refs. [9, 10].

III. Static Testing Approaches

This section presents the three methods for static testing. The goal of the static tests was to determine the nondimensional aerodynamic force and moment contributions from each control surface, over a range of variables including Mach number, dynamic pressure, angle of attack, and control surface deflections. The OFAT method is described first, followed by the DOE and QS2 methods.

A. One Factor at a Time

Traditional tests using the one factor at a time (OFAT) method involve gathering data as a single factor is changed over a predefined range while other factors are held at constant values. This process is then repeated for each factor of interest until the desired data are obtained. For the OFAT test points presented in this paper, the tunnel speed and test article angle of attack were first set. Then each control surface was moved to various positions while the remaining surfaces stayed at zero deflection. This process was repeated for each control surface, and then also for other tunnel conditions and angles of attack.

Testing using the OFAT method is commonplace in wind tunnels because a large volume of data can be quickly gathered and because tests proceed in a straightforward manner. Results are readily understood (e.g., producing a lift curve) and trends or abnormalities can be quickly discovered. Additionally, OFAT tests can quickly determine limits to a flight envelope, such as the onset of flutter. Data quality is also higher with OFAT tests which allows for the flow in the wind tunnel to reestablished after each change in the test article configuration change and or tunnel condition. The time-averaged measurements are more accurate as a result. As such, most tunnels and staff are oriented to conducting OFAT tests.

However, there are drawbacks to this approach. A large amount of data is produced and must be subsequently stored and processed. Interactions between multiple factors, such as the lift from two adjacent control surfaces, either cannot be captured or required potentially large numbers of separate tests to investigate. Systematic error and bias can be introduced into the data by sequentially varying the factors, for example due to temperature rise. And when many factors are present, OFAT testing can take a long amount of time that could be cost prohibitive.

B. Design of Experiments

To overcome several drawbacks of OFAT testing, design of experiments (DOE) methods can be used. In these static tests, multiple factors are changed at the same time and in randomized and decorrelated ways. The randomization reduces systematic errors whereas the low correlation allows for accurate characterization of the independent influence of each modeling variable. Nonlinear effects of individual factors and interactions between multiple factors can also be investigated. Some combinations of factors can be purposefully revisited during testing to help quantify uncertainty. Generally, less data are needed for DOE tests than for OFAT tests, so that tests are shorter for the same level of statistical accuracy. More information on the general approach is given in Refs. [11, 12].

Since the late 1990's, there has been an interest at NASA LaRC in using the DOE method to improve the efficiency of wind tunnel tests [13]. As vehicle configurations have increased in number of factors, these methods have been used more often and in some cases were indispensable in obtaining aerodynamic models. For example, the GL-10 urban air mobility (UAM) design had 23 factors due to a large number of control surfaces and rotating propellers. A complete OFAT test would have taken years to complete [5]. Multiple other but similar vehicles have been tested [6, 14]. Although DOE was not critical for the IAWTM tests because there were only 10 control surfaces (in addition to angle of attack and tunnel condition), the application here facilitates a useful comparison to other test techniques.

DOE tests for wind tunnels also have drawbacks. OFAT tests are usually still initially performed to check out the flight envelope, find important details in the aerodynamic responses, and determine safe and appropriate ranges for test factors. Wind tunnels are usually oriented for OFAT testing and are not always easily adapted to the randomization involved with DOE testing, which can add wear and tear on the tunnel machinery due large deflection or configuration changes. Measured data are also more difficult to interpret during the testing phase, and a deeper understanding of modeling and statistical analysis is needed to design the experiments and understand the results.

C. Quasi-Steady Sinusoids

In the OFAT and DOE tests, the control surfaces were moved to a specified set of steady deflection angles, steady data were recorded, and this process was repeated many times. A different idea is used in the quasi-steady sinusoids (QS2) approach, where all the control surfaces deflect simultaneously and move at different and slow frequencies. In this way, much of the design space is traversed, and is done so in a continuous manner rather than at discrete points.

This approach was used in Ref. [15] to automate a wind tunnel test for measuring control effectiveness. Recently, a similar idea using dynamic maneuvers with multisine inputs was combined with DOE testing to result in highly efficient wind tunnel testing of eVTOL models with many factors [16].

The main point in this test technique is to cover the design space and obtain effectively static data, similar to the OFAT and DOE tests. Because all surfaces are moving, interaction terms between factors can be investigated, as with the DOE approach. If the sinusoid with the lowest frequency has more than one cycle, then all the test points are revisited and statistical averaging and uncertainty quantification can be applied. The frequencies must be slow enough so that higher-frequency dynamics, such as unsteady aerodynamics or structural modes, are not excited by the test, or are small enough to be neglected. This limit, along with the number of control surfaces to be tested, determines the length of the QS2 test. Because the oscillation frequency for each surface is known, frequency-domain methods can also be used to analyze the data. However, it is assumed in this approach that the system is linear. Nonlinearities, for example in the drag production, could produce overlapping harmonics that would be indistinguishable from other excitation frequencies.

IV. Results

The results for this paper were taken from the first entry into the wind tunnel. The test condition was Mach 0.55, dynamic pressure 103 lbf/ft^2, and a test article angle of attack of 0 deg. These data correspond to test 679, run 18, and test points 580–593. During these test points, the OFAT, DOE, and QS2 tests were performed in sequence, in addition to other tests.

Limits for the control surface deflections are given in Table 1. These limits were bounded by loads on the actuators, and were valid up to Mach 0.80 and 200 lbf/ft^2. The hydraulic ailerons and outboard MPFG were allowed to traverse the entire ±10 deg deflection range. For the remaining MPFs, the limits are smaller, and also not symmetric about zero.

Table 1 Allowable surface deflections up to 0.8 Mach and 200 lbf/ft^2

	MPFA	MPFB	MPFC	AILA	MPFD	MPFE	MPFF	MPFG	AILB	AILC
Max., deg	+6	+5	+3	+10	+4	+5	+7	+10	+10	+10
Min., deg	−7	−6	−5	−10	−7	−8	−9	−10	−10	−10

Control surface deflection angles were not measured directly but came from potentiometer measurements internal to the servomotor actuators. Actuator commands were also recorded.

All measurements were originally recorded at 1000 Hz. The data were downsampled to 10 Hz so that the same least squares techniques, which are summarized in Appendix A, could be applied to all three analyses and to ease computation requirements. Downsampling was done by applying a global smoothing algorithm [8] with a cutoff frequency of 5 Hz, and then retaining 1 out of every 100 data points. This process reduced the effective sampling rate without introducing aliasing into the data [17].

A. One Factor at a Time

Each of the 10 test points designed using the OFAT method had a duration of 160 s. During these tests, a single surface would traverse between positive and negative deflection angles. The same deflection angles were used for each surface, but some control surfaces could only achieve a subset of those angles due to the limits given in Table 1. While one control surface was commanded to a non-zero deflection, the remaining surfaces were commanded to zero deflection. Some combinations of deflection angles were repeated. These tests were automated in that time histories of actuator commands were read from data files and did not need an operator to manually set the commands or deflections. Transitions between different set points occurred slowly, over 5 s, and portions of steady data were recorded for 7 s. In total, the OFAT tests used 1600 s or about 27 min of time collecting data. A total of 67 different steady-state data points were collected.

One example set of time histories for the control surface data is shown in Fig. 3. Only the AILA surface is moved in this data; there are nine other similar runs (which are not shown) where the other control surfaces are sequentially moved in a similar fashion. The commands are shown in blue, whereas the calibrated deflection measurements are shown in red. Note that several of the surfaces (particularly MPFC, MPFD, and MPFE) had constant offsets from the commanded deflections at zero. In general, the MPFs settled on a different steady-state value each time after being commanded to move. This resulted in different bias parameters (e.g., steady-state lift) in each static test but not the estimated control effectiveness parameters.

Figure 4 shows the corresponding aerodynamic coefficients data, downsampled to 10 Hz, in blue. The red lines are model fits, discussed below. Measurements of C_D and C_n had low values of signal-to-noise ratio (SNR), at 0.46 and 0.19 respectively, due to the smaller effects of drag. Measurements of C_L, C_l, and C_m had much larger SNR values of 3.0, 5.6, and 3.7 respectively, due to the larger effects of lift. The coefficient C_Y was not measured because the TDT uses a five-component balance.

Figure 5 shows a correlation matrix for the control surface deflections, which are labeled along the diagonal. The lower triangle shows pairwise correlation coefficients [8], which range from −1 to +1 and quantify the linear correlation between the two signals. Corresponding elements in the upper triangle show a cross-plot of the data. This plot matrix serves as a diagnostic tool in that when correlation coefficients become large in absolute value, and the cross-plots resemble a straight line, the ensuing parameter estimation becomes ill conditioned [8]. Since only one surface was moved at a time in the OFAT tests, the control surface time histories are orthogonal and correlation is not an issue for parameter estimation.

The least-squares method, which is summarized in Appendix A, was used to fit models of the aerodynamic coefficients as a function of control surface deflections. The data downsampled to 10 Hz was used, and the entire data record (including the 5 s transitions) were used to make closer comparisons to the DOE and QS2 tests. The model structure was determined using stepwise regression and multivariate orthogonal functions. Uncertainties on the estimated model parameters were corrected for colored residuals, which is an extension of the basic least-squares theory. A brief summary of these techniques is given in Appendix A, but see Refs. [7, 8] for a full explanation and software.

For the OFAT tests, the models selected for the aerodynamic coefficients were

$$C_D = C_{D_0} + \sum_{i=1}^{10} C_{D_{\delta_i}} \delta_i + \sum_{i=1}^{10} C_{D_{\delta_i^2}} \delta_i^2 \tag{1a}$$

$$C_L = C_{L_0} + \sum_{i=1}^{10} C_{L_{\delta_i}} \delta_i \tag{1b}$$

$$C_l = C_{l_0} + \sum_{i=1}^{10} C_{l_{\delta_i}} \delta_i \tag{1c}$$

$$C_m = C_{m_0} + \sum_{i=1}^{10} C_{m_{\delta_i}} \delta_i \tag{1d}$$

$$C_n = C_{n_0} + \sum_{i=1}^{10} C_{n_{\delta_i}} \delta_i + \sum_{i=1}^{10} C_{n_{\delta_i^2}} \delta_i^2 \tag{1e}$$

All models in Eq. (1) have of a bias term (e.g., C_{D_0}) and linear control derivatives for each of the control surfaces (e.g., $C_{D_{\delta_1}}$). For convenience, control surfaces are enumerated from 1 to 10 going from the wing root to wing tip, as shown in Fig. 2. Higher-order polynomial derivatives (e.g., $C_{D_{\delta_1^2}}$) were also investigated and were statistically significant only for the C_D and C_n coefficients, due to the drag production. At higher angles of attack, these and other higher-order polynomial terms can become important to the model [18].

Estimates of the unknown parameters in Eq. (1) using least squares are shown in Figs. 12 through 16. Bias parameters (e.g., C_{D_0} are given in the first subplot, linear control derivatives (e.g., $C_{D_{\delta_1}}$) are given in the second subplot, and any quadratic derivatives estimated are given in the third subplot. The blue triangle markers show the OFAT estimates, and the red error bars indicate the estimated two standard errors or 95% confidence bounds on the parameter estimates. Because different bias parameters were estimated in each OFAT test, reported bias parameters and uncertainties are the weighted arithmetic mean values from all 10 tests.

B. Design of Experiments

The DOE maneuver was designed to test 67 different data points to match the number of OFAT points. The design matrix was a cuboidal, completely randomized, I-optimal response surface design. In general, I-optimal designs minimize the integrated prediction variance across the design space for an assumed model structure [12]. The design supported a reduced cubic model structure with all possible linear, pure quadratic, and pure cubic model terms; two-factor and three-factor interaction model terms were also supported for neighboring control surfaces. The commercial software called Design-Expert®* was used to generate the test points.

The design included 66 free design points and 1 center point where all the commanded deflections were zero. Similar to the OFAT tests, control surface command time histories were read from a file and the test proceeded without further operator input. Each data point was held for 8 s, and transitions between data points occurred over 7 s. In comparison to the OFAT tests, each test point was held for 1 s longer, and transitions took an additional 2 s. This was done because larger changes in deflections were commanded in the DOE tests than the OFAT tests. In total, the DOE test lasted 1030 s, or a little over 17 minutes. A total of 67 different data points were collected.

Figure 6 shows commands and surface deflections for the DOE test. This plot shows that all surface are simultaneously being commanded to different angles throughout their range limits. Note again tracking errors in the midspan MPF surface deflections.

*The use of trademarks or names of manufacturers in this report is for accurate reporting and does not constitute an official endorsement, either expressed or implied, of such products or manufacturers by the National Aeronautics and Space Administration.

Figure 7 shows the downsampled measurements of the aerodynamic coefficients and model fits. The same aerodynamic model shown in Eq. (1) was used to fit the DOE data. First-order interaction effects between adjacent control surfaces (e.g., $C_{D_{\delta_1 \delta_2}} \delta_1 \delta_2$) were explored using stepwise regression and multivariate orthogonal functions but were not statistically significant. Similar models have been used in other works, for example Ref. [19]. Estimated parameters and uncertainties are also shown in Figs. 12 through 16 using the green circle markers.

Figure 8 shows the correlation matrix for the DOE test. The maximum pairwise correlation coefficient was 0.16 in absolute value. This is a very low number and indicates pairwise correlation is not a factor of concern for parameter estimation. The coverage of the cross-plots in the upper triangle of the matrix shows the DOE test fully spanned the control surface space, unlike in the OFAT tests.

C. Quasi-Steady Sinusoids

The QS2 test was designed to last for 900 s or about 15 min. This created a fundamental period of 900 s or 0.0011 Hz. Originally, the test was designed using harmonic frequencies, which are orthogonal. The second harmonic was assigned to the slowest moving control surface, which then had a 450 s period and 0.0022 Hz frequency. The second harmonic was the lowest used, instead of the first fundamental harmonic, in order to have two full cycles of data and facilitate data averaging. The 11th harmonic was assigned to the fastest moving control surface, which had about a 82 s period and 0.0122 Hz frequency. This upper frequency was the limiting factor that dictated the length of the test. It was desired to keep this value low to maintain quasi-static flow conditions, and to not excite responses due to unsteady aerodynamics or structural dynamics. With additional testing or analysis, this frequency could potentially be raised, which would result in a shorter overall test duration. The excitations ranged in reduced frequency k from 2.3×10^{-5} to 2.5×10^{-4}, which is approximately static according to Theodorsen theory [20].

The control surfaces were assigned a frequency corresponding to harmonics 2–11. To keep sequential harmonics from being assigned to adjacent surfaces, these were staggered so that MPFA had harmonic 2, MPFB had harmonic 7, MPFC had harmonic 3, AILA had harmonic 8, and so forth.

In generating the sinusoid commands, the minimum allowable range in Table 1 determined the amplitude. For example, with MPFD, the amplitude of the sinusoid was selected as 4 deg. Although using a piece-wise continuous sinusoid could have use different positive and negative amplitudes to better cover the design space, that type of excitation could create nonlinearities in the data, and there was a desire to conduct a linear analysis.

To guard against higher harmonics from different control surface movements overlapping, each of the ten excitation frequencies were offset by 1/10th of a harmonic. This way, both the excitation frequencies of the 10 surfaces and their first few harmonics are staggered, so that aerodynamic responses due to quasi-static and nonlinear origins can be distinguished. For this testing, it was not important that the sinusoids be orthogonal (even though pairwise correlations were very low), only that they slowly cover the design space. Harmonic numbers and frequencies are summarized in Table 2.

Table 2 Summary of quasi-steady sinusoid parameters, T = 900 s

	MPFA	MPFB	MPFC	AILA	MPFD	MPFE	MPFF	MPFG	AILB	AILC
Harmonic	2.0	7.5	3.1	8.6	4.2	9.7	5.3	10.8	6.4	11.9
Frequency, Hz	0.0022	0.0083	0.0034	0.0096	0.0047	0.0108	0.0059	0.0120	0.0071	0.0132

Figure 9 shows control surface measurements from the QS2 test. The same tracking errors with the midspan MPF surfaces are evident.

Figure 10 shows the downsampled measurements and the model fits. Higher-order control derivatives and first-order interaction effects between adjacent control surfaces were again investigated but found to not be statistically significant.

Figure 11 shows correlations for the QS2 test. The largest correlations were 0.09 in absolute value, which is small and indicates no problems with pairwise correlations. Although the parameter space was well spanned by many combinations of control surfaces (e.g., AILB and AILC), some other combinations had less coverage (e.g., MPFF and MPFG or MPFD and AILB). However, as discussed next in Section IV.D, this difference in coverage did not impact the results. Figures 12 through 16 show the model parameter estimates and uncertainties, where the QS2 results are shown as the red diamond markers.

D. Discussion

In preparing for the tests, both the OFAT and DOE tests take comparatively little time to plan. The main points to consider are number of factors to move, ranges and resolution, and feasibility of the total test time estimated. By comparison, the QS2 tests required more analysis. This included determining adequate harmonic frequencies, frequency shifting to avoid nonlinear effects, and some preliminary computational fluid dynamics (CFD) analysis to check unsteady aerodynamic effects.

The OFAT tests were designed first and used the most amount of time, primarily because only one control surface was moved at a time. The DOE tests were then designed to match the number of test points. Because this test had simultaneously changing control surfaces, the conditions were achieved more efficiently, despite using longer amounts of time for transition and steady data collection. The QS2 test was designed last and used the least amount of time. However, this again was somewhat arbitrary, as the test could be repeated (to have four full cycles of the lowest frequency instead of two) to improve noise rejection in the analysis.

The analysis used in this paper was not conventional in that the entire records of (downsampled) data were used to analyze the OFAT and DOE tests, instead of averaging the steady data first. This was done so that the same procedures could be applied to the QS2 tests data for comparison. The more conventional approaches were also applied to the OFAT and DOE test data, and resulted in similar parameter estimates and uncertainties. Other procedures based on frequency-domain analysis could be applied to the QS2 data, but were not done for this paper and will be pursued in the future.

For all of the tests, nonlinear higher-order polynomial models (up to cubic for the DOE tests) were not pursued at this time. These terms were significant for C_D and C_n due to the effects of drag, but were not significant for C_L, C_l, and C_m. The DOE and QS2 tests had the possibility for identifying first-order interaction terms between any control surfaces pairs. For this data set, however, interaction terms were negligible based on the parameter estimates and uncertainties, as well as statistical metrics including coefficient of determination, F-ratio, predicted squared error (PSE), and others [8]. It is possible that at other angles of attack, which were tested but not discussed here, those effects may become important. In addition, other OFAT tests were conducted where one control surface was moved while other control surfaces were held at non-zero deflections. At the expense of additional time for testing different surface deflection combinations, this approach could provide insight on interaction effects. This data was also not analyzed for this paper.

The cross-plots in Figs. 5 through 11 all indicated that pairwise correlations, a common problem in system identification, was not an issue. Each method overcame this issue by design. However, these plots also show the coverage of the control surface deflections. The OFAT test fully covers the range for one control surface (i.e., AILA in the plots shown). The DOE test optimized the distribution of test points to minimize the prediction variance for a predefined design model structure which included a center point and emphasized test points along the control surface boundaries. There was no effort made in the QS2 tests to cover the space, and in some cases this resulted in some combinations of control surfaces not being tested.

In all three sets of test data, effects of unsteady aerodynamics at low frequencies and effects of structural dynamics at high frequencies appear to be small. This is based on an analysis of residuals performed in the frequency domain after model fitting was performed. These effects were a concern during test preparation because moving the control surfaces can excite these dynamics, which would degrade the identified models.

In general, the parameter estimates and uncertainties reported in Figs. 12 through 16 were similar, and mostly in statistical agreement with each other. This observation supports that the test data, model structures, and analysis were adequate and consistent. For the bias parameters (e.g., C_{D_0}), the OFAT data was similar to but outside of statistical agreement with the DOE and QS2 tests. As mentioned earlier, this was due to non-zero deflections for the stationary control surfaces during the OFAT tests. Similarly, the linear derivatives for MPFC, MPFD, and MPFE had more scatter than for the other control surfaces. This was true for the linear derivatives, and to a greater extent for the quadratic derivatives, where applicable.

V. Conclusions

Static wind tunnel tests were conducted with the IAWTM half-span test article of an elongated transport-type aircraft configuration having 10 trailing-edge control surfaces. Three different tests were performed to obtain this information, and results were compared.

The first test was the standard OFAT test, where each control surface was deflected through its range while all other control surfaces remain fixed. The second test used DOE, where test points were optimized to minimize the prediction variance in a predefined model structure and randomized in a way that facilitated efficiently testing and analysis while also providing robustness to time varying instrumentation error. The third test was QS2, where each control surface moved in a slow manner to produce quasi-static measurements.

The main findings of this paper are the following:

- OFAT tests used the most time, followed by DOE and then QS2. However, there are several parameters that can be varied to change test duration and data quality.
- The DOE and QS2 facilitate estimation of nonlinear interaction effects, if they are significant. To do this with OFAT tests, a much longer amount of test time is needed to run different combinations of control surface deflections.
- In general, the estimated parameters between the three approaches were mostly consistent for the data presented and produced the same results.

Acknowledgments

This work was supported by the NASA Advanced Air Transport Technology (AATT) Project and the Advanced Air Vehicles Program (AAVP) as part of a Cooperative Agreement with Boeing. The authors would like to acknowledge significant contributions to this project and the work presented in this paper over the course of many years by team members from Boeing, NextGen Aeronautics, and NASA.

References

[1] Gipson, L., "Advanced Air Transport Technology (AATT) Project Technical Challenges," https://www.nasa.gov/aeronautics/advanced-air-transport-technology-aatt-project-technical-challenges/, accessed Nov. 2025.

[2] Heaney, P., and Quindlen, J., "Overview of the Integrated Adaptive Wing Technology Maturation Wind-Tunnel Test Objectives," AIAA Paper 2024-2509, Jan. 2024. doi:10.2514/6.2024-2509.

[3] Quindlen, J., Ortega, D., Clark, G., Hussain, H., Forte, C., Nguyen, N., Heaney, P., Bentley, P., Coulson, D., Giles, I., McHugh, G., Pinkerton, J., Ramey, J., and Stevens, W., "Summary of the Integrated Adaptive Wing Technology Maturation Wind Tunnel Tests of a High Aspect Ratio Commercial Transport Aircraft," AIAA Paper 2026-XXXX, Jan. 2026. doi:10.2514/6.2026-XXXX.

[4] Brooks, T., Kenway, G., and Martins, J., "Benchmark Aerostructural Models for the Study of Transonic Aircraft Wings," *AIAA Journal*, Vol. 56, No. 7, Jul. 2018, pp. 2840–2855. doi:10.2514/1.J056603.

[5] Murphy, P., and Landman, D., "Experiment Design for Complex VTOL Aircraft with Distributed Propulsion and Tilt Wing," AIAA Paper 2015-0017, Jan. 2015. doi:10.2514/6.2015-0017.

[6] Simmons, B., and Murphy, P., "Aero-Propulsive Modeling for Tilt-Wing, Distributed Propulsion Aircraft Using Wind Tunnel Data," *Journal of Aircraft*, Vol. 59, No. 5, Sep.–Oct. 2022, pp. 1162–11. doi:10.2514/1.C036351.

[7] Morelli, E., "System IDentification Programs for AirCraft (SIDPAC)," version 4.1, NASA Software Catalog, https://software.nasa.gov/software/LAR-16100-1, accessed Dec. 2025.

[8] Morelli, E., and Klein, V., *Aircraft System Identification: Theory and Practice*, 2nd ed., Sunflyte Enterprises, Williamsburg, VA, 2016.

[9] Cole, S., Noll, T., and Perry, B., "Transonic Dynamics Tunnel Aeroelastic Testing in Support of Aircraft Development," *Journal of Aircraft*, Vol. 40, No. 5, Sep. 2003, pp. 820–831. doi:10.2514/2.6873.

[10] Ivanco, T., "Unique Testing Capabilities of the NASA Langley Transonic Dynamics Tunnel, an Exercise in Aeroelastic Scaling," AIAA Paper 2013-2625, Jun. 2013. doi:10.2514/6.2013-2625.

[11] Montgomery, D., *Design and Analysis of Experiments*, 10th ed., John Wiley & Sons, Hoboken, NJ, 2019.

[12] Myers, R., Montgomery, D., and Anderson-Cook, C., *Response Surface Methodology: Process and Product Optimization Using Designed Experiments*, 4th ed., John Wiley & Sons, Hoboken, NJ, 2016.

[13] DeLoach, R., "Applications of Modern Experiment Design to Wind Tunnel Testing at NASA Langley Research Center," AIAA Paper 98-0713, Jan. 1998. doi:10.2514/6.1998-713.

[14] Simmons, B., and Busan, R., "Statistical Wind-Tunnel Experimentation Advancements for eVTOL Aircraft Aero-Propulsive Model Development," AIAA Paper 2024-2482, Jan. 2024. doi:10.2514/6.2024-2482.

[15] Grauer, J., "Modeling and System Identification of an Ornithopter Flight Dynamics Model," Ph.D. thesis, University of Maryland, 2012.

[16] Simmons, B., Morelli, E., Busan, R., Hatke, D., and O'Neal, A., "Aero-Propulsive Modeling for eVTOL Aircraft Using Wind Tunnel Testing with Multisine Inputs," AIAA Paper 2022-3603, Jun.–Jul. 2022. doi:10.2514/6.2022-3603.

[17] Hardin, J., "Introduction to Time Series Analysis," NASA RP-1145, Mar. 1986.

[18] Nguyen, N., Cramer, N., Hashemi, K., Ting, E., Drew, M., Wise, R., Boskovic, J., Precup, N., Mundt, T., and Livne, E., "Real-Time Adaptive Draft Minimization Wind Tunnel Investigation of a Flexible Wing with Variable Camber Continuous Trailing Edge Flap System," AIAA Paper 2019-3156, Jun. 2019. doi:10.2514/6.2019-3156.

[19] Xiong, J., Nguyen, N., and Bartels, R., "Study of Trailing Edge Mini-Plain Flap Interactions on a Wind Tunnel Scale Aspect Ratio 13.5 Common Research Model," AIAA Paper 2025-0873, Jan. 2025. doi:10.2514/6.2025-0873.

[20] Leishman, J., *Principles of Helicopter Aerodynamics*, 2nd ed., Cambridge University Press, New York, NY, 2006.

A. Least-Squares Estimation

This appendix provides a brief summary of some of the analysis techniques used in this paper. Full details can be found in Ref. [8] and the supporting references, and software can be requested at the website given in Ref. [7].

In the ordinary least-squares (OLS) approach, the $N \times 1$ array of measurements $\mathbf{z}$ are modeled as

$$\mathbf{z} = \mathbf{y} + \mathbf{v} \tag{2a}$$

$$= \mathbf{X}\boldsymbol{\theta} + \mathbf{v} \tag{2b}$$

where $\mathbf{y}$ is the model output, $\mathbf{v}$ is zero-mean, Gaussian white measurement noise, $\mathbf{X}$ is the matrix of regressors or independent modeling variables, and $\boldsymbol{\theta}$ is an array of model parameters to be estimated.

The least-squares approach minimizes the cost function

$$J = \frac{1}{2}\boldsymbol{\nu}^T\boldsymbol{\nu} \tag{3}$$

where

$$\boldsymbol{\nu} = \mathbf{z} - \mathbf{y} \tag{4}$$

are the model residuals, which are the differences between the measurements and the model output for those measurements. The solution for the model parameters that minimize the cost in Eq. (3) is

$$\hat{\boldsymbol{\theta}} = \left(\mathbf{X}^T\mathbf{X}\right)^{-1}\mathbf{X}^T\mathbf{z} \tag{5}$$

The uncertainties for the estimated parameters are

$$\text{cov}(\hat{\boldsymbol{\theta}}) = E\left[\left(\hat{\boldsymbol{\theta}} - \boldsymbol{\theta}\right)\left(\hat{\boldsymbol{\theta}} - \boldsymbol{\theta}\right)^T\right] \tag{6a}$$

$$= \sigma^2\left(\mathbf{X}^T\mathbf{X}\right)^{-1} \tag{6b}$$

where the equation-error variance σ^2 is typically estimated from the model residuals as

$$\hat{\sigma}^2 = \frac{\boldsymbol{\nu}^T\boldsymbol{\nu}}{N - n_p} \tag{7}$$

where N is the number of measurements and n_p is the number of parameters estimated. Equations (2) through (6) are implemented in the SIDPAC function `lesq.m`.

The standard OLS problem assumes the residuals are white. In practice, the estimated uncertainties are typically too small because they do not account for colored residuals that contain frequency content from neglected dynamics. Therefore, a correction to the uncertainties is typically performed based on the autocorrelation of the residuals. This increases the uncertainty bound but does not alter the parameter estimate. This is implemented in the SIDPAC function `r_colores.m`.

Equation (2) assumes a perfect model structure. In other words, $\mathbf{X}$ contains all the necessary independent variable and is perfectly known. In practice, this is not always the case and several techniques can be used. One is called stepwise regression. This is where regressors are iteratively substituted into and out of the model structure, the least squares solution is produced, and a variety of statistical metrics are evaluated. This is implemented in the SIDPAC function `swr.m`. A second approach is called multivariate orthogonal functions. Here, a pool of candidate regressors are evaluated. A Gram-Schmidt process is applied to orthogonalize the regressors, which decouples the least-squares problem so regressors can be included into the problem in the order for which they decrease the residuals. This is implemented in the SIDPAC function `mof.m`.

B. Plots

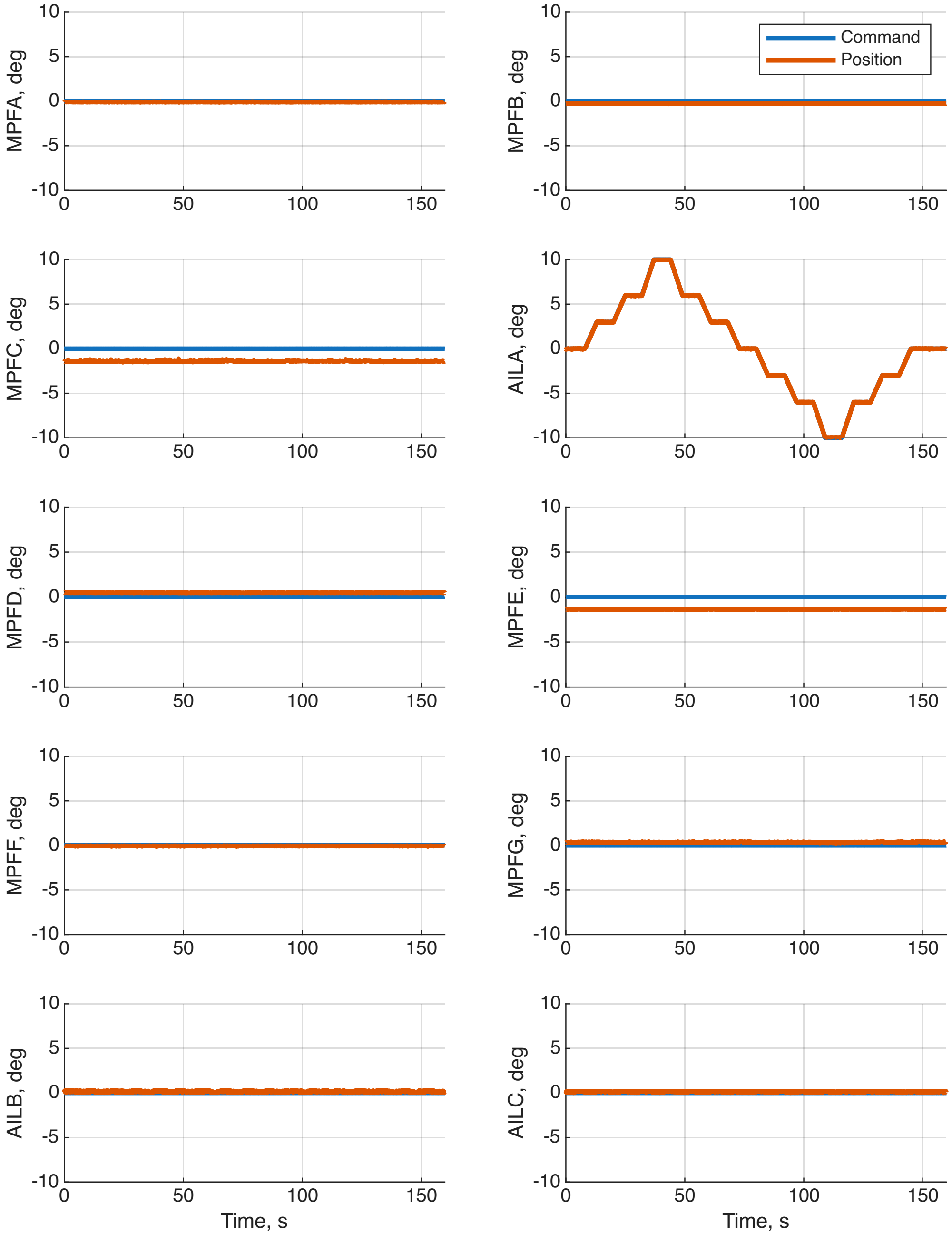

Fig. 3 Control surface commands and positions for AILA OFAT test.

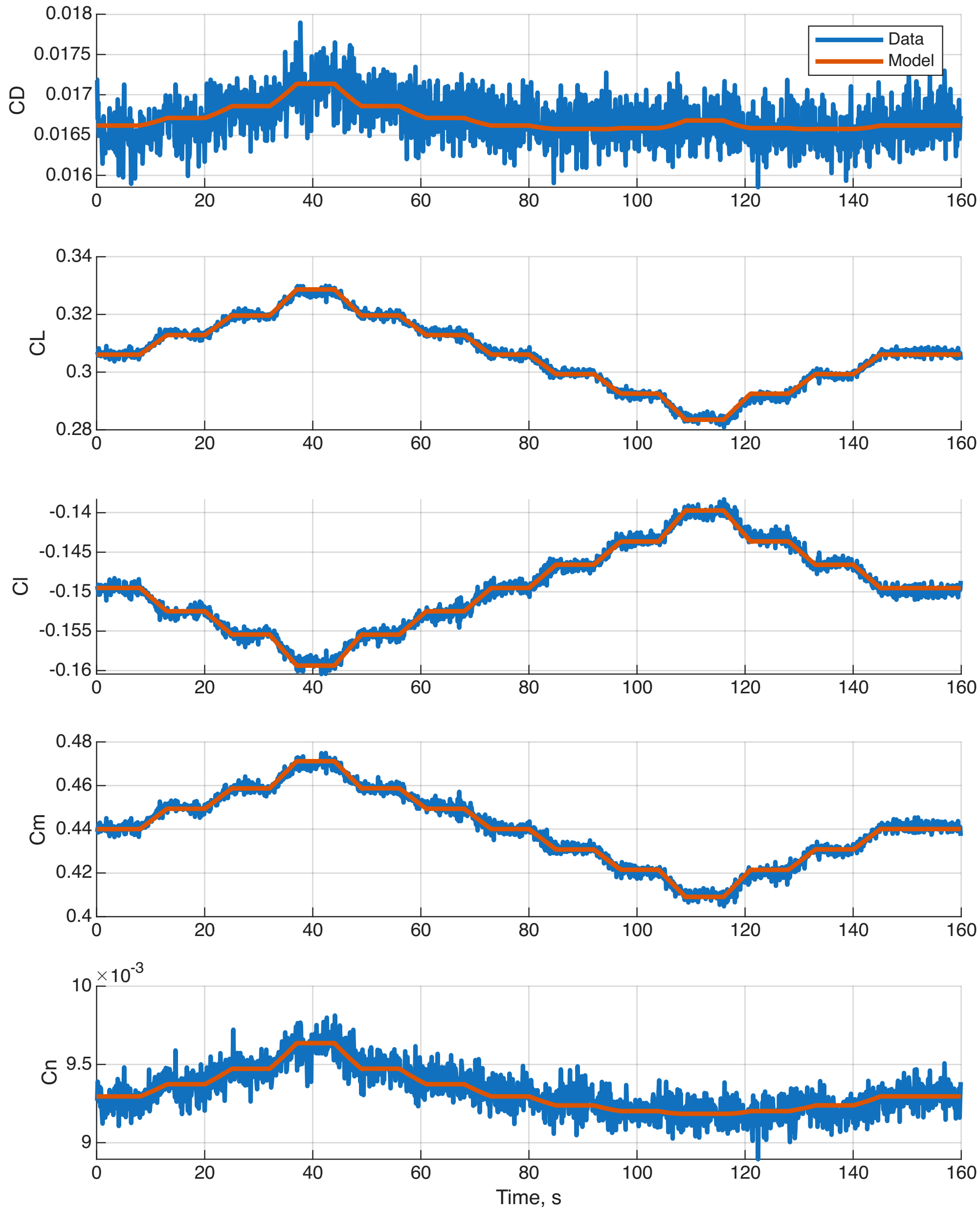

Fig. 4 Aerodynamic force and moment coefficients for AILA OFAT test.

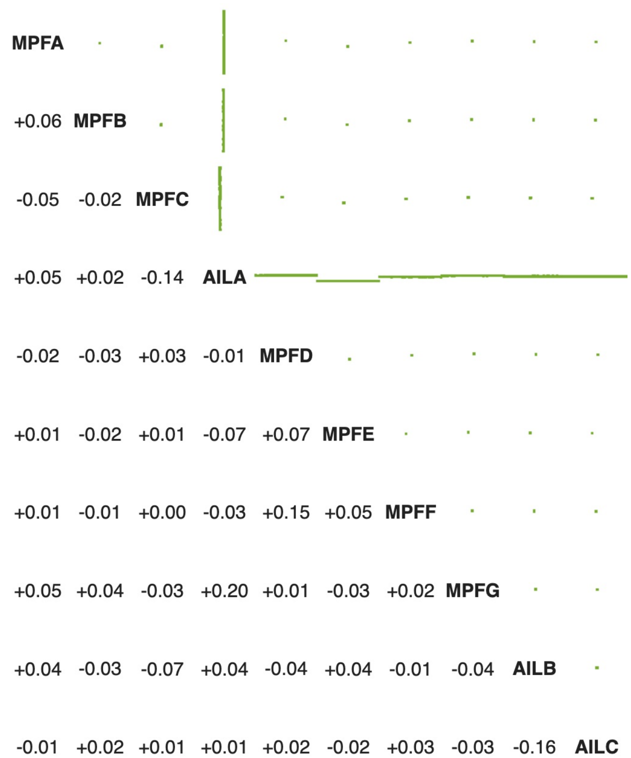

Fig. 5 Correlation cross-plots of surface positions for AILA OFAT test.

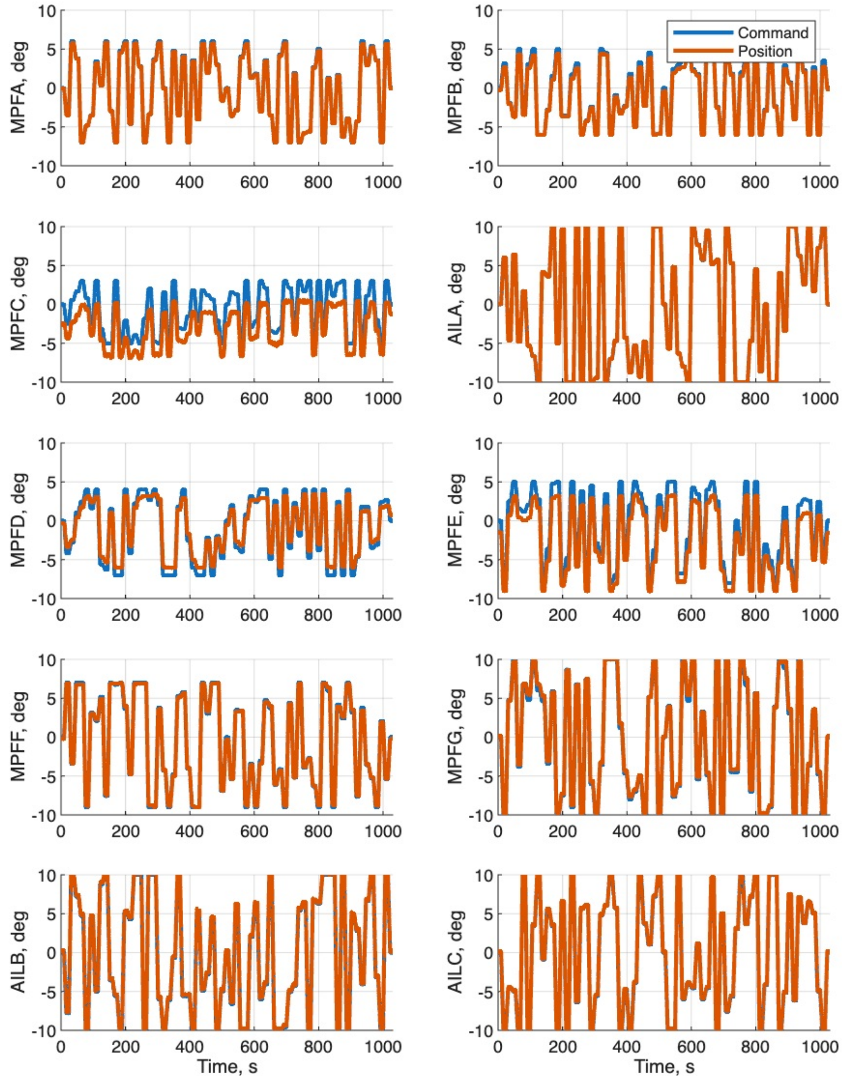

Fig. 6 Control surface commands and positions for DOE test.

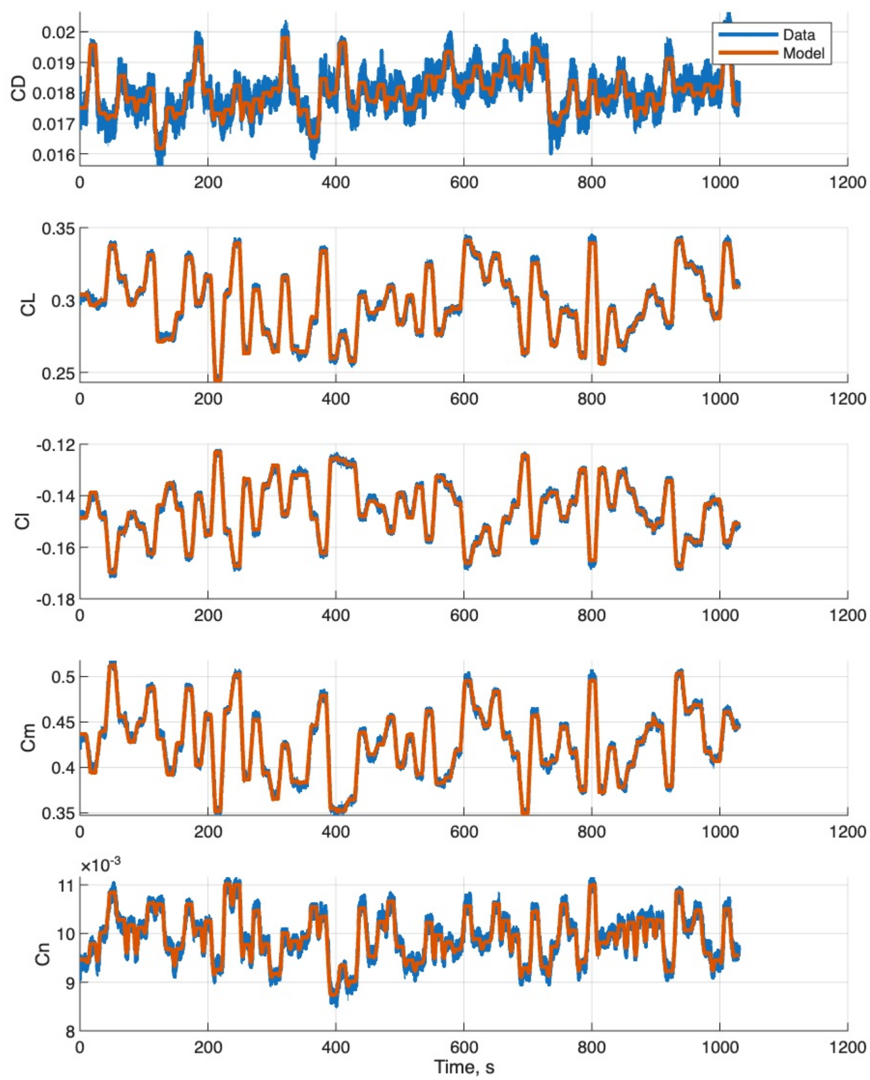

Fig. 7 Aerodynamic force and moment coefficients for DOE test.

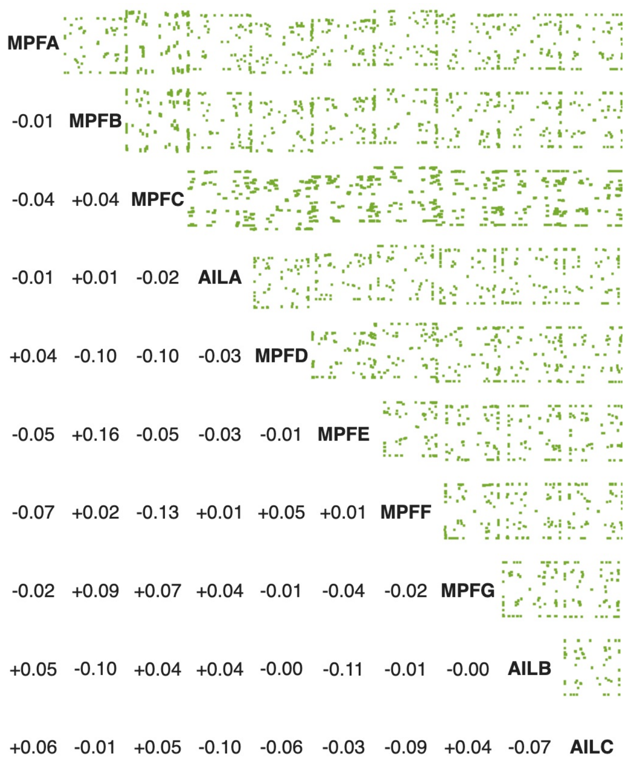

Fig. 8 Correlation cross-plots of surface positions for DOE test.

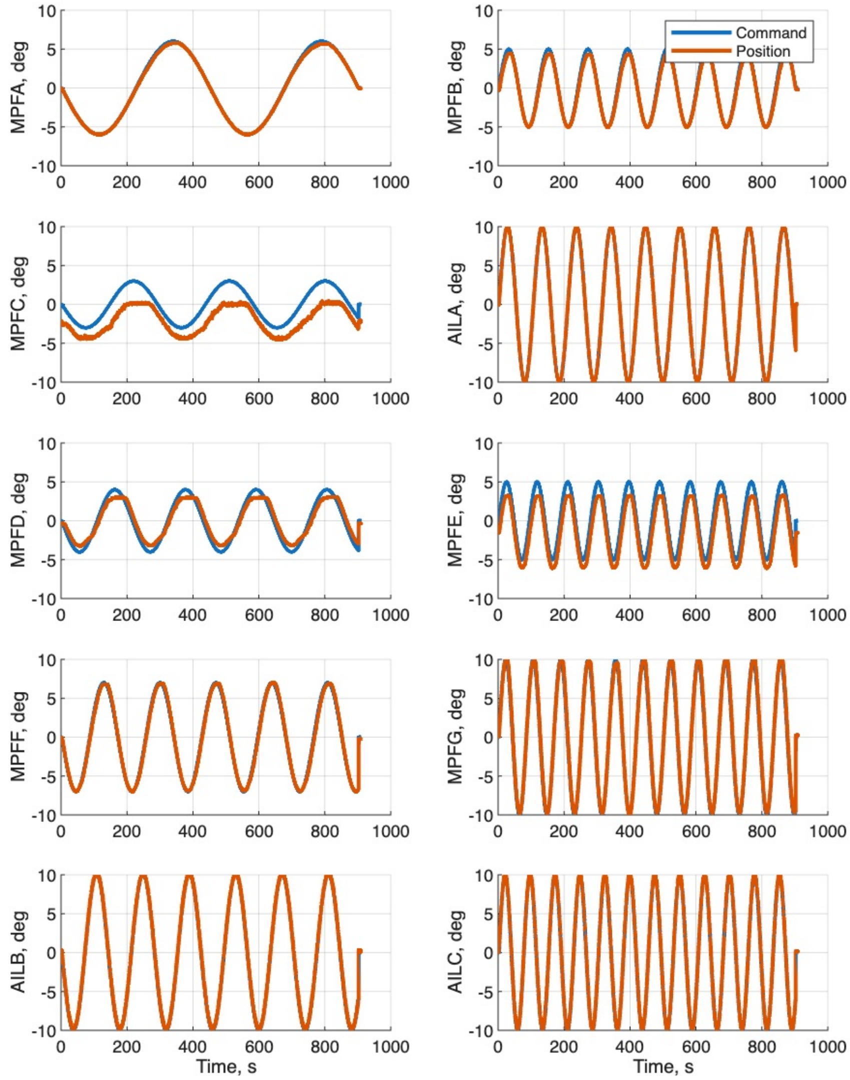

Fig. 9 Control surface commands and positions for QS2 test.

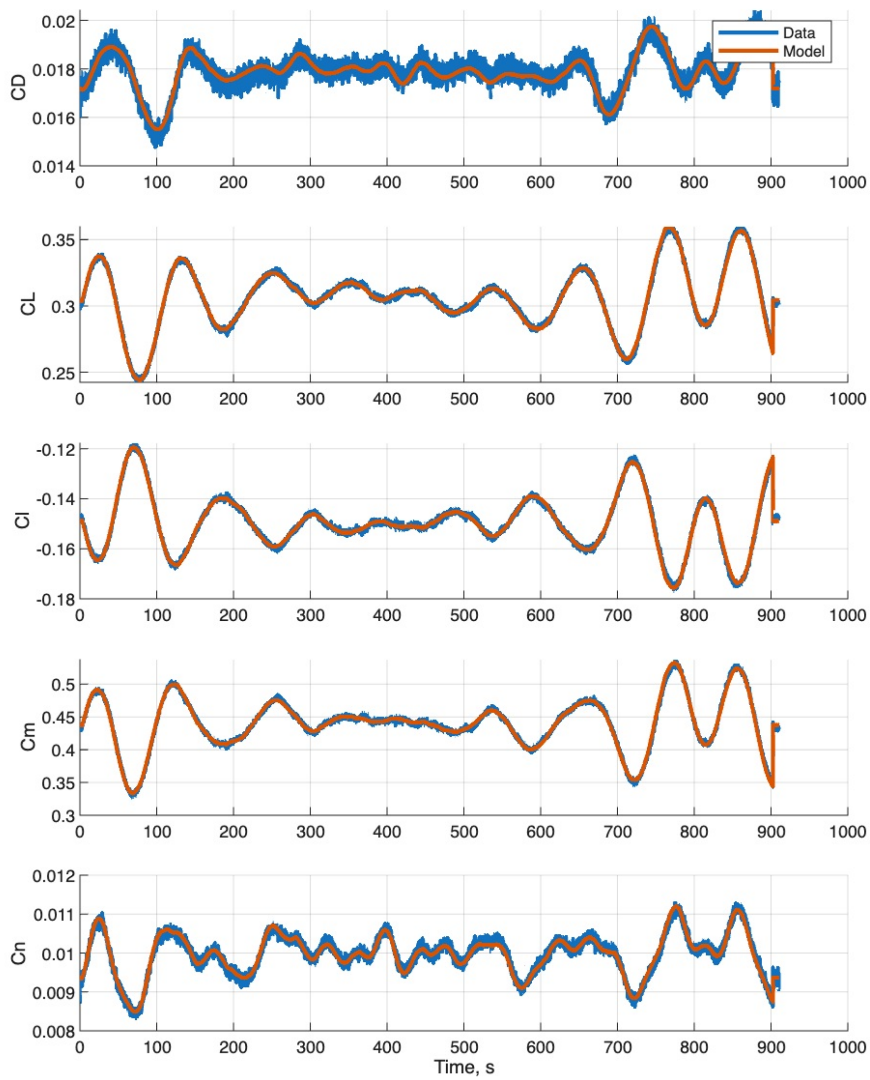

Fig. 10 Aerodynamic force and moment coefficients for QS2 test.

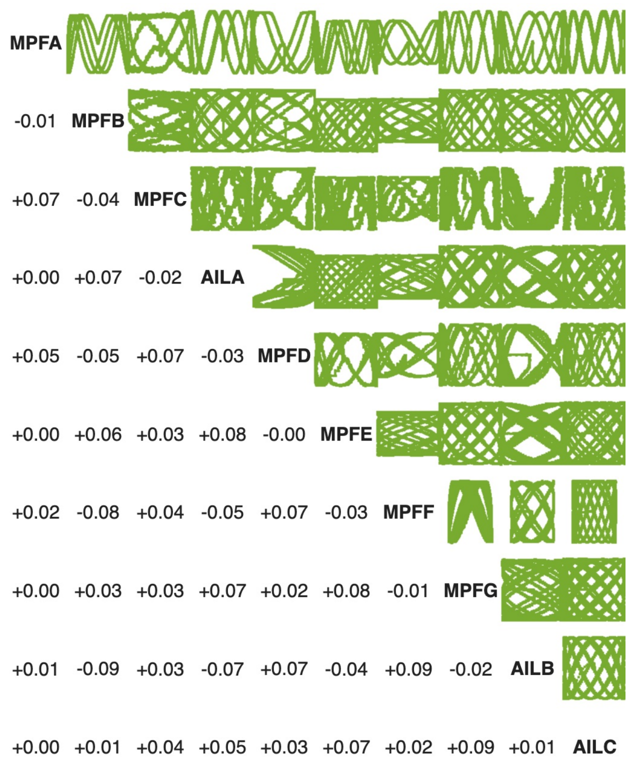

Fig. 11 Correlation cross-plots of surface positions for QS2 test.

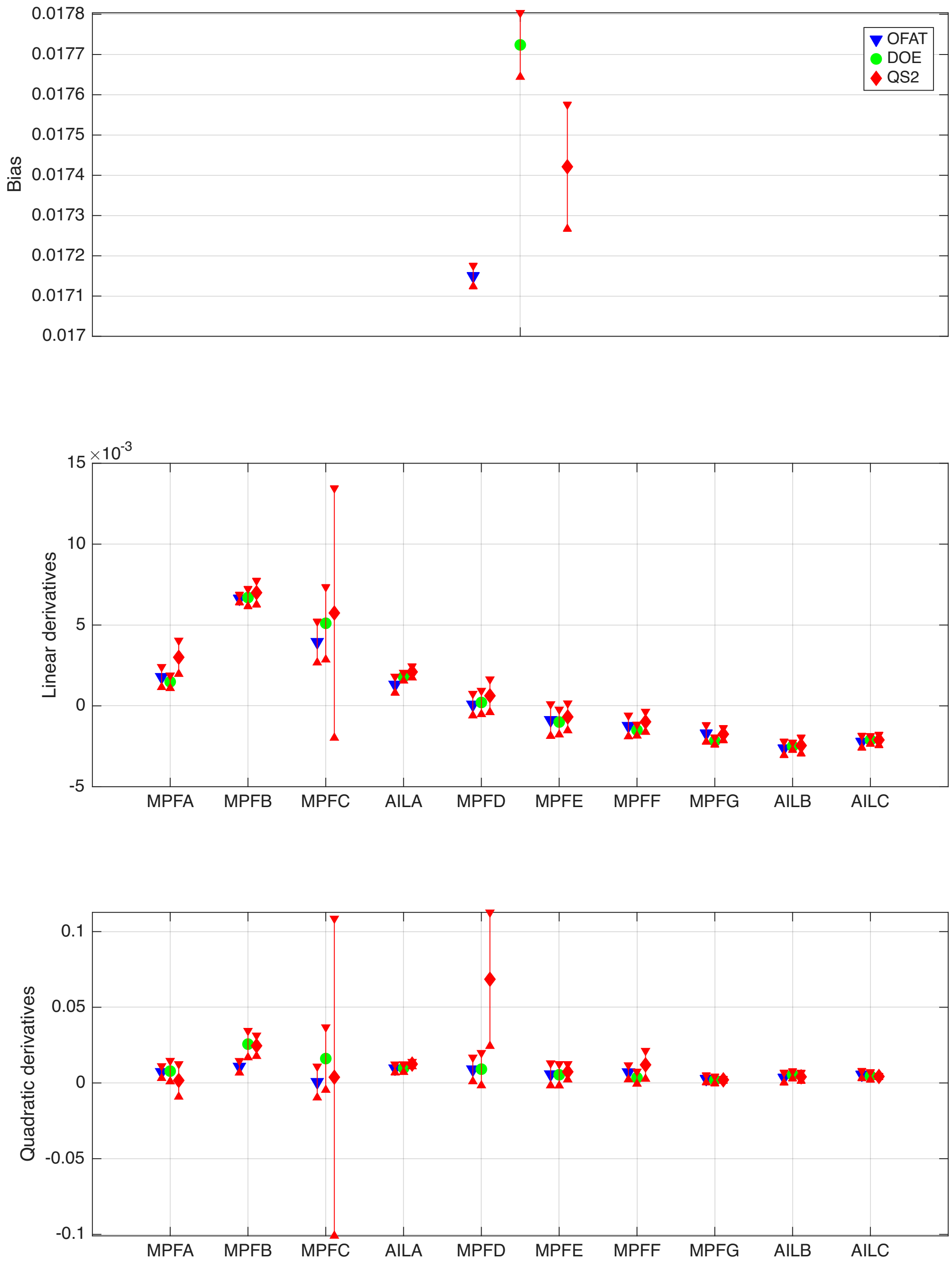

Fig. 12 Drag force coefficient parameters and uncertainties.

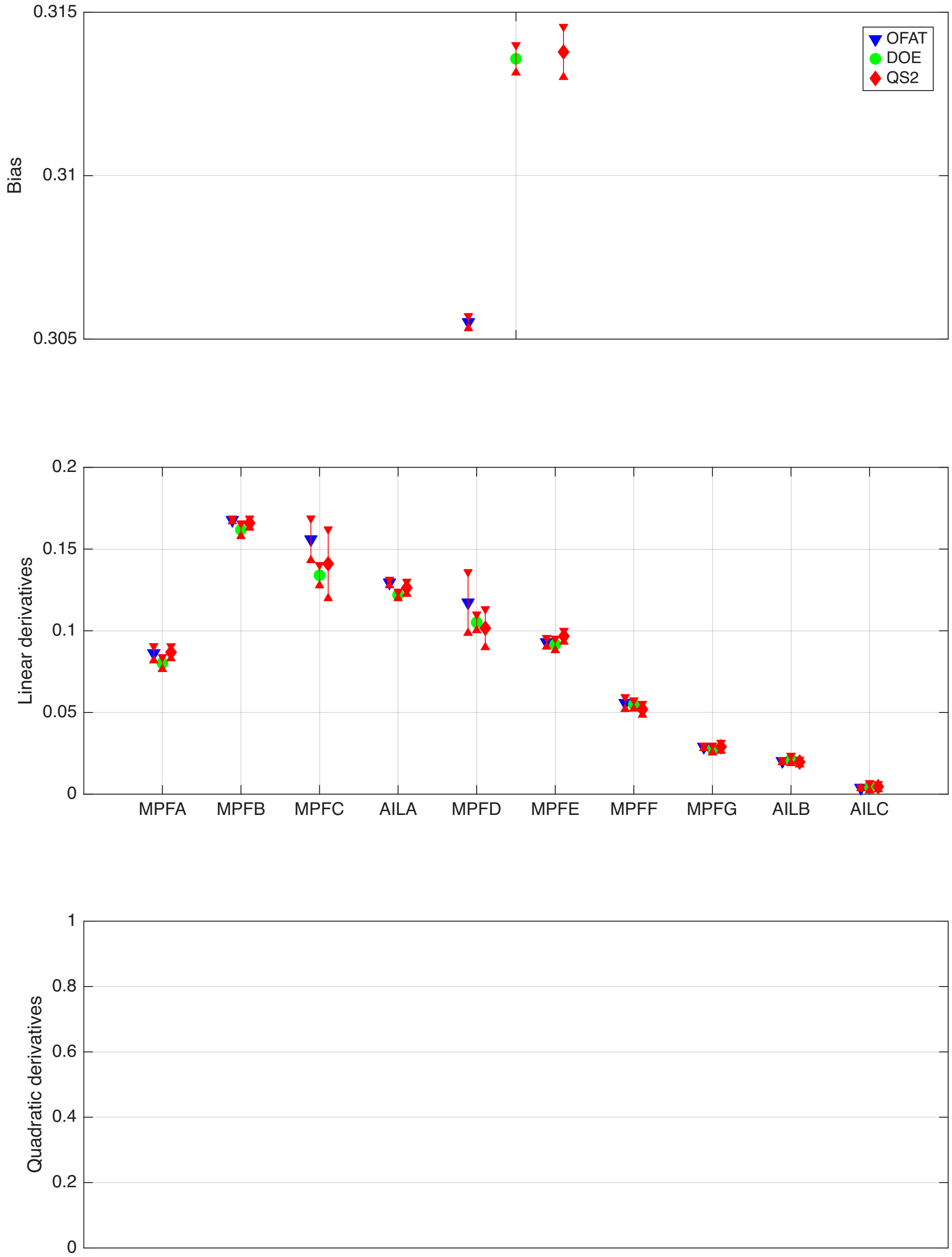

Fig. 13 Lift force coefficient parameters and uncertainties.

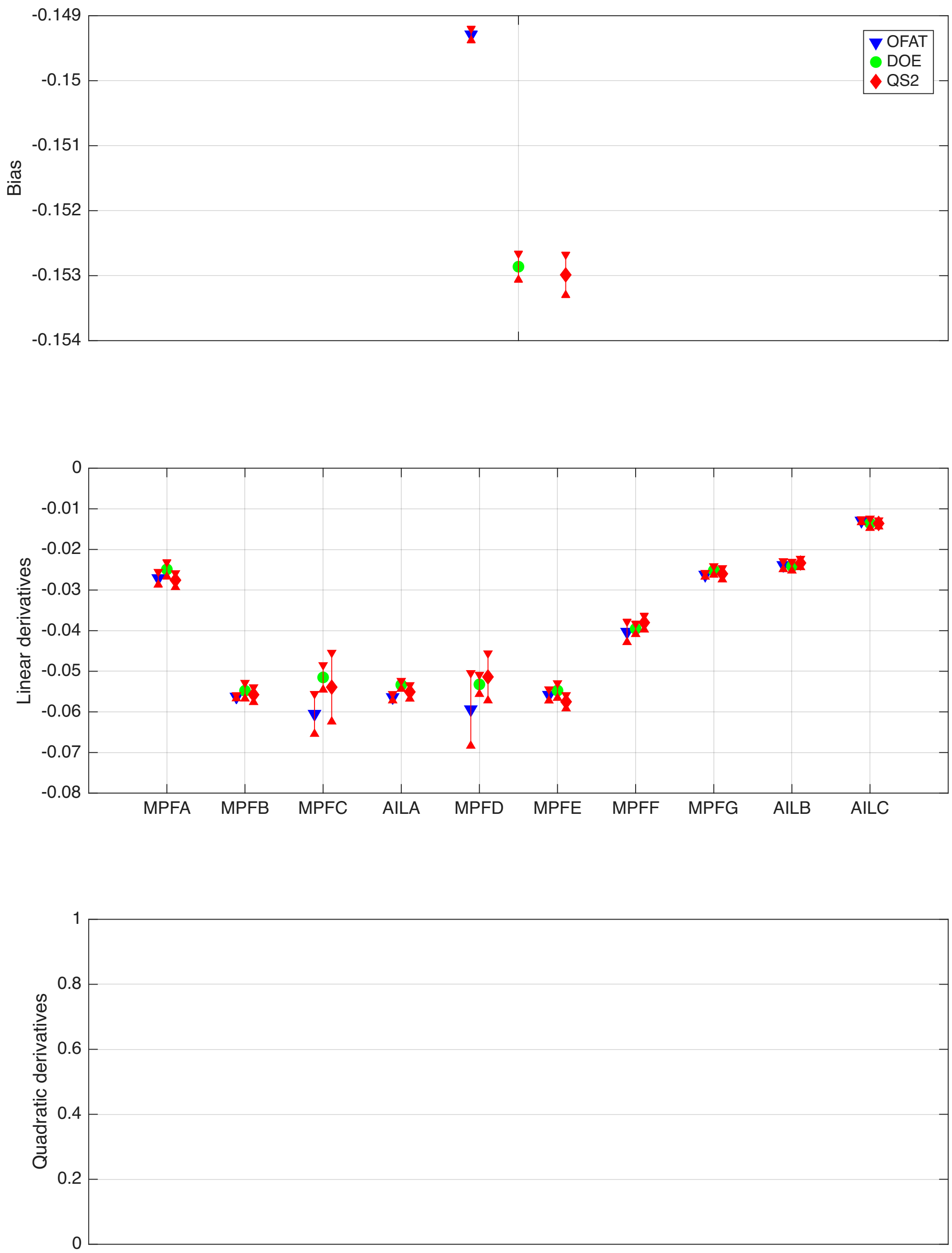

Fig. 14 Roll moment coefficient parameters and uncertainties.

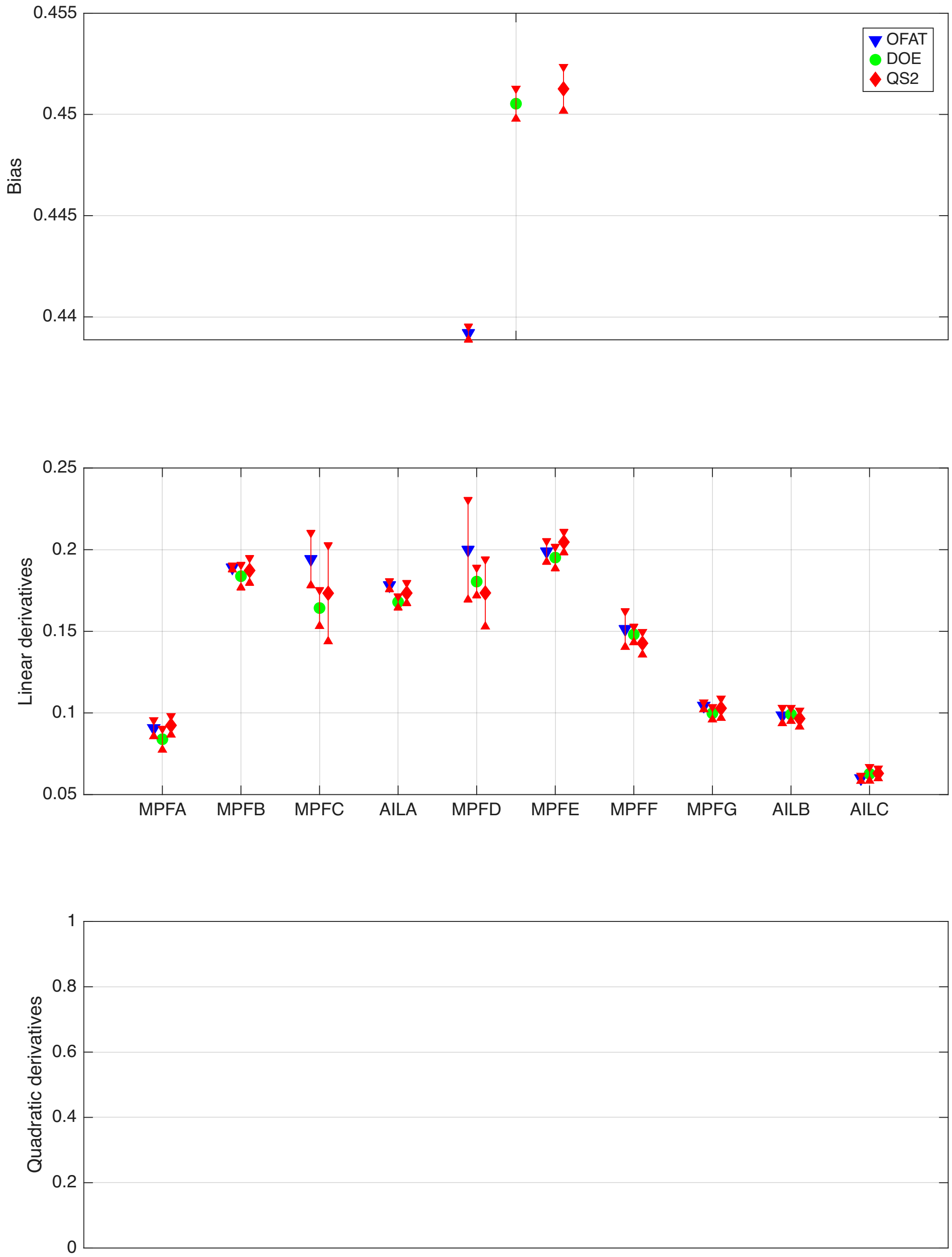

Fig. 15 Pitch moment coefficient parameters and uncertainties.

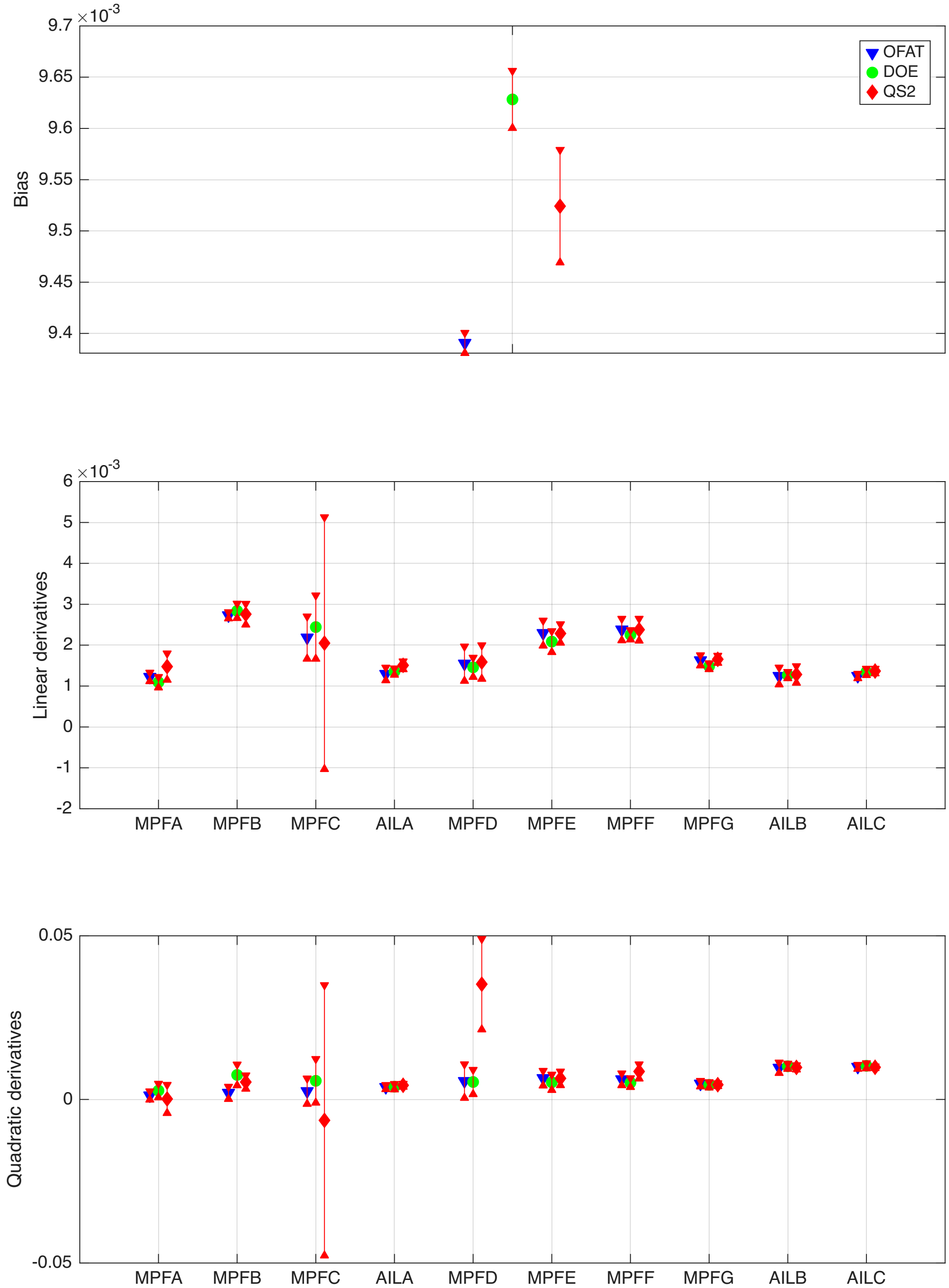

Fig. 16 Yaw moment coefficient parameters and uncertainties.